Fish and Shellfish Immunology 92 (2019) 508–518

Contents lists available at ScienceDirect

Fish and Shellfish Immunology

journal homepage: www.elsevier.com/locate/fsi

Full length article

Elevated biosynthesis of palmitic acid is required for zebrafish against *Edwardsiella tarda* infection

Di Xu[a], Jie Wang[a], Chang Guo[a], Xuan-xian Peng[a,b,c], Hui Li[a,b,c,*]

[a] Center for Proteomics and Metabolomics, State Key Laboratory of Bio-Control, Sun Yat-sen University, University City, Guangzhou, 510006, People's Republic of China
[b] Laboratory for Marine Biology and Biotechnology, Qingdao National Laboratory for Marine Science and Technology, Qingdao, 266071, People's Republic of China
[c] Southern Marine Science and Engineering Guangdong Laboratory (Zhuhai), Zhuhai, 519000, People's Republic of China

ARTICLE INFO

Keywords:
Edwardsiella tarda
Inactivated vaccine
Metabolomics
Innate immunity
Biosynthesis of unsaturated fatty acids
TCA cycle

ABSTRACT

Mechanisms by which vaccines enhance immunity to combat bacterial pathogens are not fully understood. Recently, we have found that live *Edwardsiella tarda* vaccine enhances ability against the bacterial challenge by metabolic modulation in zebrafish. Here we first explored the metabolic modulation promoted by inactivated *E. tarda* to eliminate the pathogen. Inactivated *E. tarda* vaccine modulated a similar metabolome to combat with the pathogen in zebrafish as live *E. tarda* vaccine did. Specifically, both vaccines promoted biosynthesis of unsaturated fatty acids and the TCA cycle. However, due to relatively higher activated TCA cycle in inactivated vaccine than live vaccine, live vaccine promoted higher abundance of palmitate than inactivated vaccine. Consistently, the protection against *E. tarda* challenge was palmitate dose-dependent. Live vaccine activated higher expression of IL-1β, IL-8,Cox-2 genes and lower expression of IL-15, IL-21 genes than inactivated vaccine, which is similar to the results stimulated by high and low doses of palmitate, respectively. These findings indicate live and inactivated *E. tarda* vaccines stimulate differential abundances of palmitate that contribute to differential innate immunities against bacterial infection. Thus, metabolic environment contributes to immune response.

1. Introduction

Edwardsiella tarda is a Gram-negative bacterium of the Enterobacteriaceae family. The pathogen infects a wide range of freshwater and marine fish, implicating in significant losses in aquaculture facilities worldwide [1–3]. Antibiotics such as tetracycline and kanamycin are effective in killing the pathogen. However, overuse and misuse of the antibiotics presents a significant challenge for its control by the existing drugs and thereby multidrug-resistant *E. tarda* has been frequently isolated from fish and human [4–6]. Vaccination is an alternative approach to prevent bacterial infection with high protection efficiency and less side effect, but now no commercial vaccines are available for the control of this bacterium although several vaccines are under preparation [7–10]. In this regard, further understanding for action mechanisms of vaccines is helpful in development of the vaccines.

A line of evidence has indicated that bacterial vaccines offer the potential to prime a naïve immune system and establish a pathogen-specific protective immunological memory and thus to represent a highly valid preventive strategy in the fight against infectious disease [11,12]. They can serve as an essential fulcrum initiating innate immunity while molding and sustaining adaptive immunity. The activated innate immunity includes complement system, lysozyme, natural killer cells, neutrophils, and macrophages, and can be harnessed in conjunction with adaptive T cell strategies [11,12]. The induced adaptive immunity contains two important immune phenotypes: (1) a bacterium-specific B-cell response with production of neutralizing antibodies with the help of a T helper cell type 2 memory and/or (2) a bacterial-specific CTL and T helper cell type 1 memory [12,13]. The bacterial vaccines have several types including dead or live organisms. Generally, higher protective efficacy is detected in the live vaccine than the dead vaccine, although both induce the innate immunity and adaptive immunity [14,15]. However, mechanisms by which live vaccine exhibits the higher protective efficacy are still elusive and wait for further investigation.

Metabolism modulates immunity to combat bacterial pathogens has been revealed [16–18]. However, whether metabolic modulation also contributes to the immune protective efficacy of vaccines is largely unknown. Recently, we have used gas chromatography/mass spectrometry (GC-MS) based metabolic profile to trace metabolic mechanisms

* Corresponding author. School of Life Sciences, Sun Yat-sen University, University City, Guangzhou, 510006, People's Republic of China.
E-mail address: lihui32@sysu.edu.cn (H. Li).

https://doi.org/10.1016/j.fsi.2019.06.041
Received 9 May 2019; Received in revised form 22 June 2019; Accepted 23 June 2019
Available online 25 June 2019

in zebrafish (*Dario rerio*) in response to live *E. tarda* vaccine. We have provided evidence that the vaccination promotes the biosynthesis of unsaturated fatty acids to combat *E. tarda* infection [19]. Meanwhile, we have shown that glucose is suppressed in tilapias infected by *E. tarda*, and exogenous glucose greatly enhances their survival ability against this pathogen [20], which is attributed to the promotion of palmitic acid and stearic acid biosynthesis [21]. These findings lead to the conclusion that metabolic regulation contributes to innate immunity against infection caused by *E. tarda*, where the elevated biosynthesis of unsaturated fatty acids is crucial. However, we do not understand why higher immune protection is detected in live than inactivated *E. tarda* vaccines based on metabolic modulation to innate immunity. The present study characterizes the metabolic difference between live and inactivated vaccines and understands whether the difference contributes to differential immunities between the two types of *E. tarda* vaccines.

2. Materials and methods

2.1. Ethics statement

All work was conducted in strict accordance with the recommendations of the Guide for the Care and Use of Laboratory Animals of the National Institutes of Health. The protocol was approved by the Institutional Animal Care and Use Committee of Sun Yat-sen University (Animal Welfare Assurance Number: I6).

2.2. Bacterial strain, culture and vaccine preparation

E. tarda EIB202 (CCTCC No. M208068) used in this study was obtained from Professor YX Zhang, East China University of Science and Technology, which was isolated from diseased turbot (*Scophthalmus maximus*) with a 44 Kb plasmid encoding three drug-resistant genes, *tetA*, *tetR* and *catA* [22]. A single colony of *E. tarda* EIB202 was picked from a tryptic soy broth (TSB) plate and propagated overnight in 5 mL TSB medium at 200 rpm (Sky-111B, SuKun, China) at 30 °C. Aliquot 1 mL culture was diluted 1:100 into fresh TSB medium and grown at 30 °C. Bacterial cells were harvested at an OD_{600} of 1.0 by centrifugation at 6,000 g (Universal 32R; Hettich Zentrifugen, Tuttlingen, Germany) for 5 min at 4 °C. The resulting cells were washed three times with saline solution as live vaccine or then resuspended in saline solution containing 1% formaldehyde and incubated at 30 °C for 24 h for inactivated vaccine. Bacterial pellets were collected as inactivated vaccine through the same centrifugation above and washing three times with sterile saline. Plate counting was used to examine bacterial sterility and purity.

2.3. Zebrafish and treatments

Zebrafish (*Danio rerio*) with approximately 3 cm long and 0.3 g body weight were obtained from Guangzhou Zebrafish Breeding Base and were free of *E. tarda* infection through microbiological detection. They were kept in aerated aquaria with a water recirculation system at 30 °C. The fish were acclimated to the animal facility for two weeks and were fed a basal diet. The animals were divided into two groups, intramuscularly injected with either 5 μL saline solution or inactivated vaccine with 500 cells without any adjuvant, each fish, which was the same cell amount as the live vaccine [19]. Eight fish each group were sampled for GC-MS analysis at 48 h post the vaccination. Meanwhile, 40 fish each group were challenged by *E. tarda* EIB202 with intraperitoneal inoculation of 1.5×10^4 CFU/fish, 5 μL per fish and observed for 14 days.

2.4. Sample preparation for GC-MS

Sample preparation for GC-MS was carried out as previously described [19]. Sampled animals in the experimental and control groups were rinsed with distilled water and then wiped thoroughly with sterilized filter paper. They were weighted and then cut into 0.5 cm long pieces on ice. Saline solution (1 mL/g body weight) was added to these pooled pieces. Tubes were vortexed at 4 °C and then centrifuged at 8,000 g for 5 min at 4 °C for collection of humoral fluid. The resulting supernatant was transferred to a new tube. GC-MS samples were prepared as described previously [23]. In brief, 100 μL humoral fluid was quenched with 200 μL ice-cold methanol (Thermo fisher) and 3 μL100 μg/mL ribitol (Sigma) was added as an internal standard. After centrifugation at 12,000 g for 10 min, the resulting supernatant was transferred and dried in a vacuum centrifuge (Labconco Corporation, Kansas City, MO, USA) for 2 h. The dried samples were used for GC-MS analysis. Eight biological samples with two technical repeats were separately used for test and control groups.

2.5. GC-MS analysis

Derivatization was carried out on the two-stage steps as described previously [24]. Briefly, 80 μL of 20 mg/mL methoxyamine hydrochloride in pyridine (Sigma) was added to the extracts and incubated for 1.5 h at 37 °C. This was followed by the addition of 80 μL *N*-methyl-*N*-trimethylsilyltrifluoroacetamide (Sigma) for another 0.5 h at 37 °C. The samples were centrifuged at 12,000 g for 10 min at 4 °C. The samples were analyzed by DSQ II GC/MS (Thermo Scientific, Austin, TX, USA). The injector temperature was kept at 270 °C. An aliquot of 0.1 μL was injected (splitless) into a column (30 m length, 0.25 mm inner diameter and 0.25 μm film thickness). Temperature program of the GC oven was 85 °C for 5.5 min, then 5 °C/min to 285 °C for 0 min, then 20 °C/min to 310 °C for 1 min, with a total run time of 48.25 min. Helium was used as carrier gas and its flow rate was 1 mL/min. Electron impact ionization was achieved at 70 eV. The ion source temperature was set at 250 °C. The MS interface temperature was held constant at 270 °C. Quadrupole temperature was 150 °C. The MS was operated using full scan mode. The mass scanning range was from 33 to 600 amu.

2.6. GC-MS data acquisition and normalization

Data acquisition contained compound identification, compound quantification, sample alignment, and peak merging. NIST MS search 2.0 and XCalibur 2.1 software were used for mass spectra library search and peak picking, respectively. The hits were assessed by rank and score. Scores from 600 to 999 were acceptable [25]. Corrected hit ranked first with a score bigger than 600. Ninety-nine compounds excluded ribitol were identified. Single ion was used for deconvolution of overlapping peaks. Relative abundance of peaks showed the number of ions [26]. After peak picking, peaks from different samples were aligned by retention time and mass spectrum. Peaks with the same compound name were merged. Data normalization included two steps. First, data matrix was normalized to ribitol. Second, individual metabolites in each sample subtracted the median and were scaled by the interquartile range of all metabolites in that sample [27]. The resulting file was used for subsequent analyses.

2.7. Statistical analysis

SPSS 13.0 was used for statistical analysis. Statistical difference was obtained by Mann-Whitney *U* test. Mann-Whitney *U* test didn't consider whether the variances of samples were equal. A p value smaller than 0.05 was considered statistically significant. P values were used to compute false discovery rates (FDR). FDR showed the proportion of true null hypotheses in the data and could be calculated in the R package "q-value" [28].

Differential metabolites and their corresponding abundances were used to Z-value analysis. Each value in control samples subtracted the mean and divided the standard deviation of the entire population from

control samples. Each value from vaccination samples subtracted the mean and divided the standard deviation of the entire population from control samples.

Differential metabolites were used for pathway enrichment analysis. MetaboAnalyst 2.0 was used to determine enriched pathways [29]. Only differential abundance of metabolites was uploaded to server. Pathway library of *Danio rerio* was selected. Hypergeometric test was selected for over-representation analysis. It was to test if metabolites involved in a particular pathway were represented more than expected by chance. Significance was set to $P < 0.05$.

Differential metabolites and their corresponding intensities were used to multivariate data analysis. Orthogonal partial least square discriminant analysis (OPLS-DA) was carried out using SIMCA 12.0 (Umetrics, Umeå, Sweden). The data scale conversion mode was Ctr-formatted (Mean-Centered scaling) processing prior to fitting. The performance of model was evaluated by $R^2 X$ (0.994), $R^2 Y$ (0.973) and $Q_{(cum)}{}^2$ (0.888). $R^2 X$ and $R^2 Y$ showed the cumulative sum of squares of all the X and Y values, respectively. $Q_{(cum)}{}^2$ showed cross-validated predictive ability.

2.8. Measurement of NADH

NADH was measured using the EnzyChrom NAD/NADH Assay Kit (BioAssay Systems) accordance with the manufacturer's instruction. The data were obtained using an ELx 808 Ultra microplate reader (Bio-Tek Instruments, Winooski, VT, USA) at OD 340 nm. The samples were analyzed in three biological repeats. GraphPad Prism v5.01 (La Jolla, CA, USA) was used to draw the scatter plot.

2.9. Addition of palmitate and propandioic acid and bacterial challenge

Zebrafish were acclimatized for 14 days at 28 °C and randomly divided into control and test groups. For complementation of palmitate, 30 individuals were included in each group. These fish were injected individually with either 5 μL of 10% BSA or palmitic acid (14 μg or 28 μg) (Sigma) dissolved in 5 μL of 10% BSA, once daily for 3 days. For injection of propandioic acid (Sigma), 25 zebrafish were included in each group. These fish were injected individually with either 5 μL of saline solution or propandioic acid (1 mM μg or 2 mM) dissolved in 5 μL of saline solution. These fish were challenged by intraperitoneal inoculation of 2.0×10^4 CFU/fish of *E. tarda* EIB202 at 24 h after the treatments and observed twice daily for 16 days for accumulative death rate.

2.10. Measurement of enzyme activity

Activity of α-Ketoglutarate dehydrogenase (KGDH), succinate dehydrogenase (SDH) and malate dehydrogenase (MDH) was measured as previously described [30].

2.11. Quantitative real-time PCR (qRT-PCR)

qRT-PCR was performed as previously described [31]. One-hundred twenty *Danio rerio* were randomly divided into two groups for detection of innate immunity genes, sixty each group. The first group included three sub-groups. Control group was injected by 10 μL 10% bovine serum albumin (BSA, fatty free) (w/v) and other two sub-groups were separately injected 14 μg and 28 μg palmitic acid as test groups. The second group also had three sub-groups. Control was injected with 10 μL saline solution and the other sub-groups were separately injected 10 μL 500 CFU of live or inactivated vaccines, respectively. The six sub-groups were injected once daily for 3 days. Total RNA was extracted from *Danio rerio* spleens using TRIZOL reagent (Ambion Life Technologies) according to the manufacturer's protocol. Four spleens were pooled as one biological sample. There were five biological replicates for each subgroup. RT-PCR was carried out on 1 μg total RNA with PrimeScript RT reagent kit with gDNA eraser (Takara, Japan) according to manufacturer's instructions. qRT-PCR was performed on a Light-Cycler 480 system (Roche, Germany) and SYBRPremix Ex TaqTM II (Takara, Japan). The cycling parameters were listed as follows: 95 °C for 30 s to activate the polymerase; 40 cycles of 95 °C for 10 s; 60 °C for 30 s; Fluorescence measurements were performed at 70 °C for 1 s during each cycle. Cycling was terminated at 95 °C with a calefactive velocity of 5 °C per second and a melting curve was obtained. Gene-specific primers used for qRT-PCR are shown in Table 1. The relative expression of each immune-related gene was calculated by $2^{-\Delta\Delta Ct}$ method using β-actin as reference gene.

Table 1
Primers for qRT-PCR.

Gene	Primer	Sequence (5′-3′)
Il-10	Forward	CTCTGCTCACGCTTCTTC
	Reverse	TCATCGTTGGACTCATAAAAC
Il-15	Forward	AAGCTCCACAGCACACTTGT
	Reverse	ACCACCCCTGGTGAGTCTTC
Il-21	Forward	CTAAAGTGCTGCACCTGTCAG
	Reverse	TTGCACTGAGCTTTCTGTGTC
Il-1β	Forward	TGGACTTCGCAGCACAAAATG
	Reverse	GTTCACTTCACGCTCTTGGATG
Il-6	Forward	ATCCGCTCAGAAAACAGTGCT
	Reverse	GTCGCCAAGGAGACTCTTTAC
Il-8	Forward	CACGCTGTCGCTGCATTG
	Reverse	GTCATCAAGGTGGCAATGATCTC
cox2	Forward	TTCTTCGCCCAGCATTTCTC
	Reverse	AATGTGCCCCAGATCCACT
β-actin	Forward	ACCCAGACATCAGGGAGTG
	Reverse	CATCCCAGTTGGTCACAATAC

3. Results

3.1. Metabolic profiling of zebrafish in response to inactivated E. tarda vaccine

First, we investigated metabolic profiling of zebrafish in response to inactivated *E. tarda* vaccine since the metabolic profile of the fish exposed to live *E. tarda* vaccine is available [19]. To do this, zebrafish were immunized by inactivated *E. tarda* vaccine as test group and injected with saline solution as a control group. Each group was divided into subgroups I and II for survival investigation and GC-MS analysis, respectively, as outlined in Fig. 1A. For the survival investigation, accumulating death showed that the inactivated vaccine reduced percent death from 72.5% to 57.5% (Fig. 1B). For the GC-MS analysis, humoral fluids were collected at 48 h post the vaccination and then used for the analysis of GC-MS. Typical total ion current chromatograms (TIC) of the two groups of samples were showed in Fig. 1C. Reliability of the detection technology was determined through a correlation coefficient between two technical repeats. Scatter plot showed metabolite abundance of two technical repeats with a minimum correlation coefficient (0.993) (Fig. 1D). A total of sixty-five metabolites were detected for each sample, which is equal to metabolites detected in zebrafish in response to live vaccine in our previous report [19]. The metabolites were classified into four categories according to their biological roles. They were 37% amino acids, 43% carbohydrates, 11% lipids, and 9% nucleotides (Fig. 1E). Global profile of metabolites was visualized as a heatmap (Fig. 1F).

3.2. Differential metabolic profiling of zebrafish in response to inactivated E. tarda vaccine

We used a two-sided Mann-Whitney *U* test to determine differential abundance of metabolites for the differential metabolome in response to inactivated vaccine compared with control. Forty-four (67.69%) metabolites out of the sixty-five metabolites identified were differential

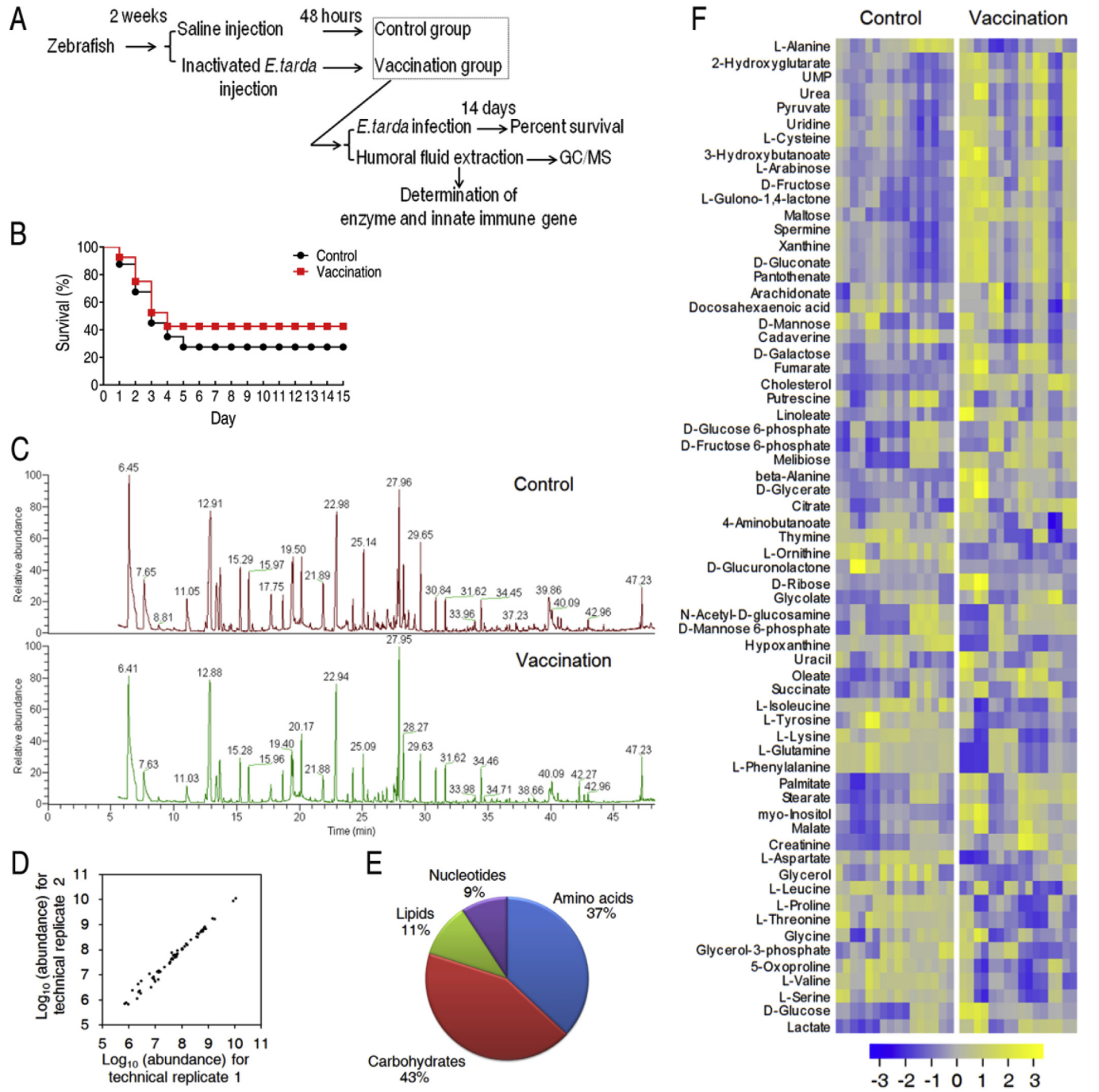

Fig. 1. Study design outline and metabolomic profiling of *Danio rerio* humoral fluid. (A) Study design outline. (B) Survival curves of zebrafish that are challenged by *E. tarda*. (C) Representative total ion current chromatograms. (D) Reproducibility of metabolic profiling platform. This plot shows two technical replicates with the weakest Pearson correlation coefficient. (E) Category of detected metabolites. (F) Heat map representation of variant metabolite levels (rows). Yellow and blue indicate increase and decrease of the metabolites, respectively. (For interpretation of the references to color in this figure legend, the reader is referred to the Web version of this article.)

at $p < 0.05$ (Chi-square test), corresponding to an FDR of 0.25%. Heatmap displayed the abundance of differential metabolites (Fig. 2A). Z-score plot spanned from −6.3 to 11.5 in inactivated vaccine (Fig. 2B). Seventeen metabolites were decreased and twenty-seven metabolites were elevated in inactivated vaccine. Compared with differential abundance of metabolites induced by live vaccine [19], forty-one metabolites shared by the two treatments, where seventeen were decreased and twenty- four were increased. In addition, two and three metabolites increased only in live and inactivated vaccines, respectively (Fig. 2C). For understanding characteristic features contributed to inactivated *E. tarda* vaccine, we investigated numbers of differential abundance of metabolites according to metabolic categories on biological roles (Fig. 2D). Out of the four categories, carbohydrates and amino acids ranked as the first two largest altered categories and then lipids and nucleotides (Fig. 2D), which is the same as live vaccine did [19]. Since differential metabolites behaved up-regulation or down-regulation, we further investigated the behaviors in each category. Higher decrease numbers than increase numbers were detected in category amino acids ($p < 0.01$, Fisher's exact test), while higher increase numbers than decrease numbers were found in categories

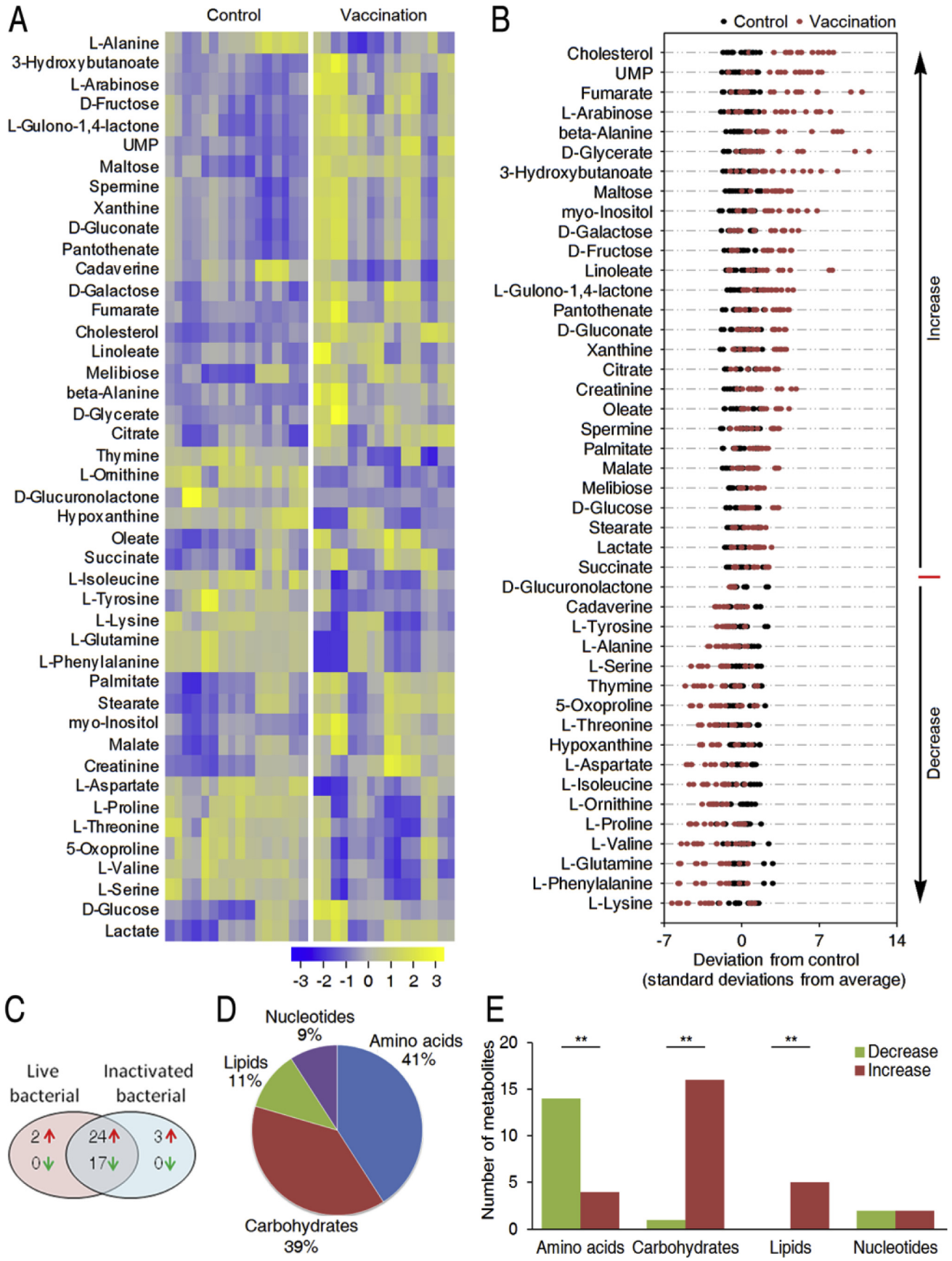

Fig. 2. Differential metabolomics in response to vaccine stimulation. (A) Heat map representation of differential metabolite levels (rows). (B) Z-score plot of differential metabolites. Each point indicates one metabolite in one technical repeat and colored by sample types. (C) Comparison of differential metabolites induced by live bacteria and inactivated bacteria. (D) The proportion of differential metabolites in four categories. (E) The number of increased and decreased metabolites in different categories. ** $P < 0.01$.

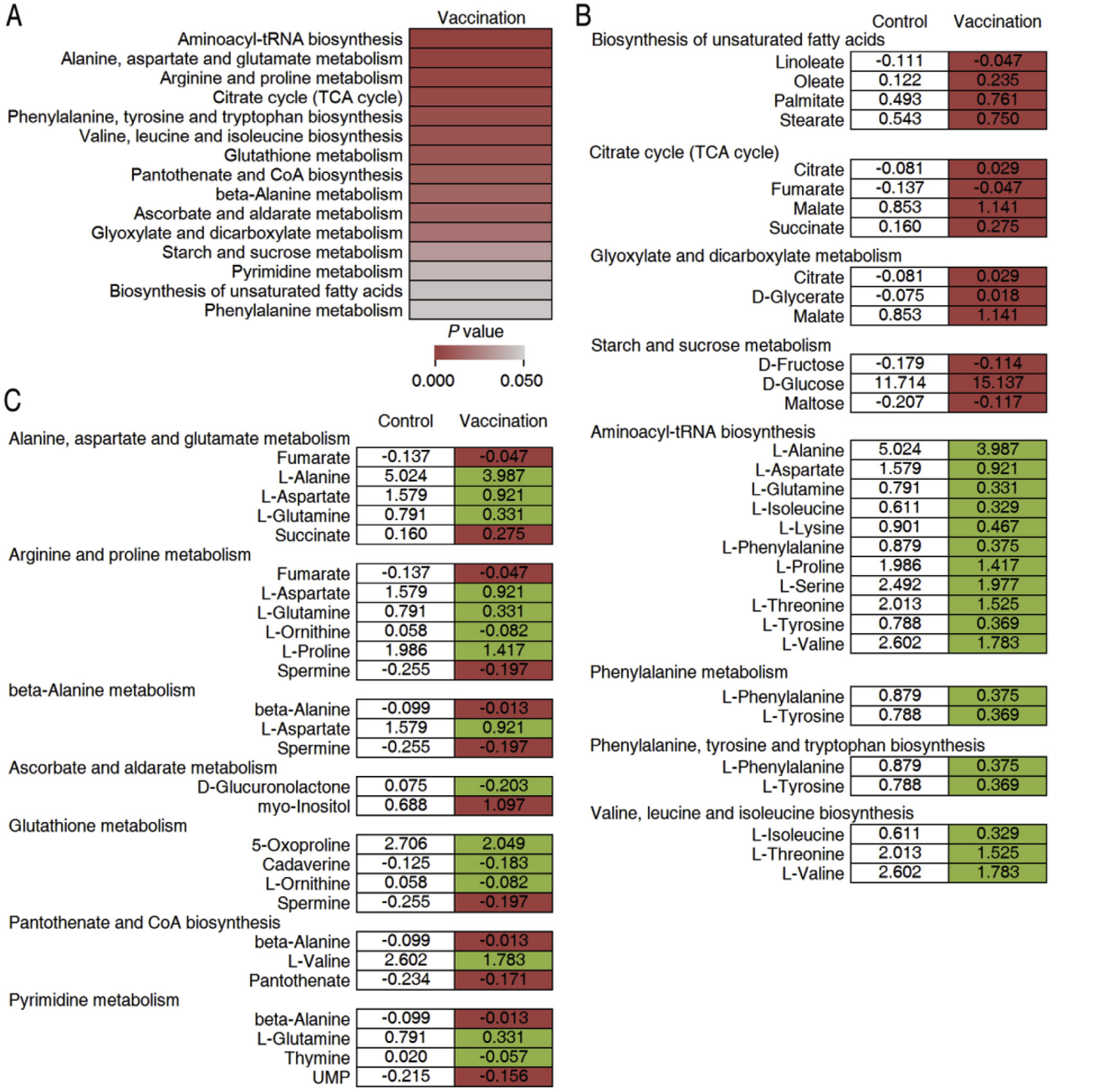

Fig. 3. Stress pattern of differential metabolites. (A) Significance of enriched pathways. (B and C) Integrative analysis of metabolites enriched in biologically meaningful pathways. The number shows the average concentration of metabolites. Red and green filled colors represent increase and decrease of the metabolites compared with control, respectively. (For interpretation of the references to color in this figure legend, the reader is referred to the Web version of this article.

carbohydrates and lipids ($p < 0.01$, Fisher's exact test) (Fig. 2E), which is the same as live vaccine did [19]. These results indicate that inactivated *E. tarda* vaccine modulates metabolism, which is related to metabolic categories. The finding that almost of metabolites and their categories overlapped between the inactivated and live vaccines suggests that the host mounts a similar metabolic strategy to respond to the two types of vaccines.

3.3. Identification of metabolic pathways in response to inactivated E. tarda vaccines

Pathway enrichment analysis was used to characterize pathways contributed to the response to inactivated vaccine. Sixteen pathways were enriched, where fifteen pathways were shared with those identified in live *E. tarda* vaccine [19]. These shared pathways were aminoacyl-tRNA biosynthesis, alanine, aspartate and glutamate metabolism, arginine and proline metabolism, citrate cycle (TCA cycle), phenylalanine, tyrosine and tryptophan biosynthesis, valine, leucine and isoleucine biosynthesis, glutathione metabolism, pantothenate and CoA biosynthesis, beta-Alanine metabolism, ascorbate and aldarate metabolism, glyoxylate and dicarboxylate metabolism, starch and sucrose metabolism, pyrimidine metabolism, biosynthesis of unsaturated fatty acids and phenylalanine metabolism (Fig. 3A). All metabolites were increased in the four enriched pathways including biosynthesis of unsaturated fatty acids, TCA cycle, glyoxylate and dicarboxylate metabolism and starch and sucrose metabolism, while all metabolites were decreased in the four enriched pathways including aminoacyl-tRNA biosynthesis, phenylalanine metabolism, phenylalanine, tyrosine and

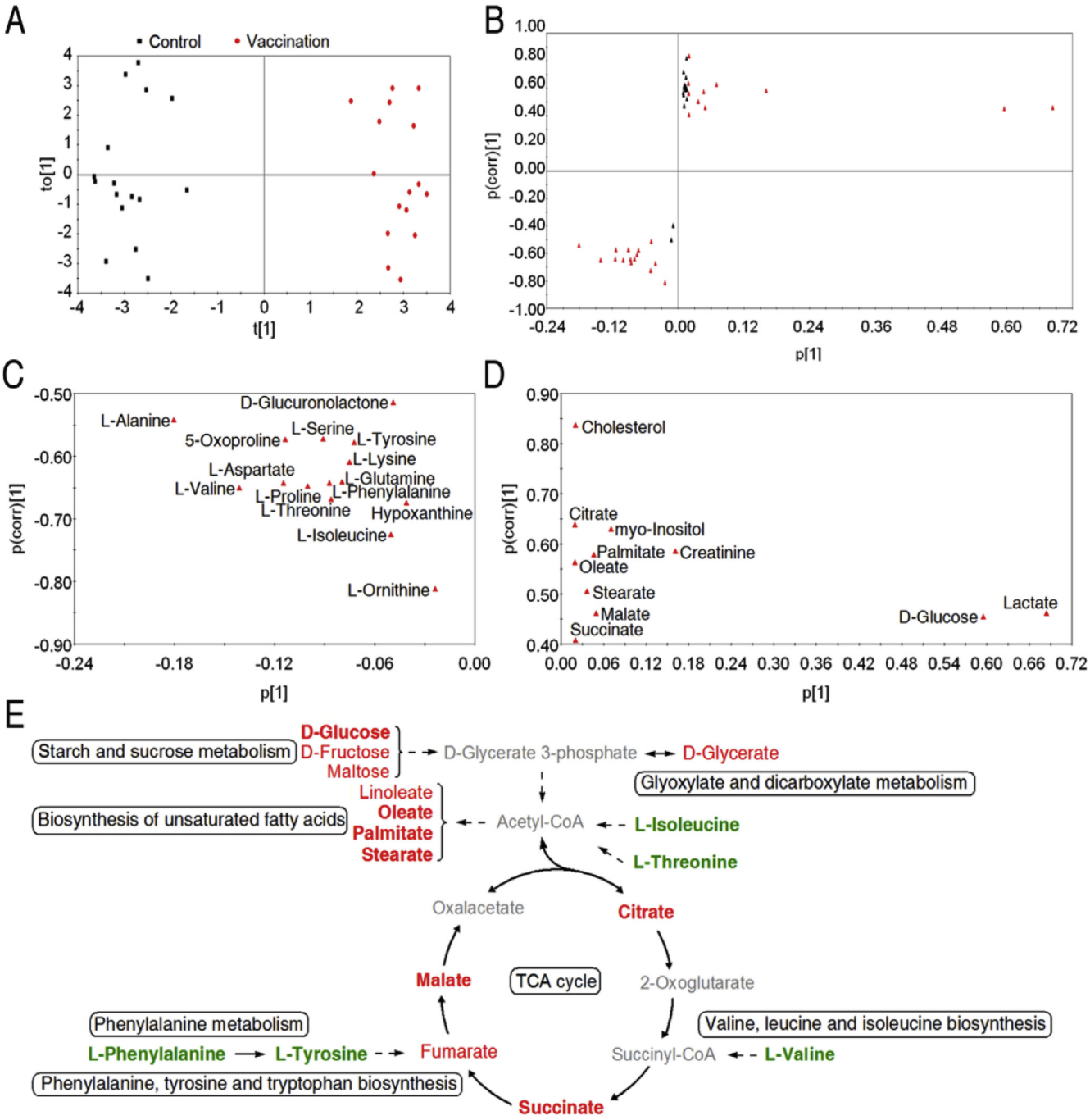

Fig. 4. Multivariate data analysis and meta-analysis of spectral data from *Danio rerio* humoral fluid. (A) Scores plot of the orthogonal partial least squares-discriminant analysis (OPLS-DA) model. (B) S-plot of the OPLS-DA model. Triangles represent metabolites. Red triangles highlight candidate biomarkers. (C and D) Display candidate biomarkers from Fig. 4B. (E) Meta-analysis of differential metabolites discriminated vaccination from control. The metabolites are colored by type of change (black, no change, red, up-regulation, green, down-regulation, gray, undetected). The metabolites in bold font are candidate biomarkers. (For interpretation of the references to color in this figure legend, the reader is referred to the Web version of this article.)

tryptophan biosynthesis, and valine, leucine and isoleucine biosynthesis (Fig. 3B). This indicates the eight pathways are crucial pathways. However, decreased metabolites and increased metabolites were simultaneously observed in the other seven pathways (Fig. 3C). These data indicate that the two vaccines modulate metabolic pathways in a similar way.

3.4. Identification of metabolic biomarkers using multivariate analysis

Supervised OPLS-DA was used to identify potential biomarkers differentiating inactivated vaccine from control. Developed model resulted in one predictive and seven orthogonal components. Predictive component focused towards variation related to class separation, while orthogonal components were uncorrelated variation. OPLS-DA scores plot showed samples within each group clustered together and a good separation between vaccination group and control group. This confirmed metabolic pattern is related to treatment. Predictive component 1 (t [1]) and orthogonal component 1 (to Ref. [1]) explained 22.71% and 49.52% of R^2 X variations, respectively (Fig. 4A). S-plot was used for identification of discriminatory variables. Cut-off values were set as

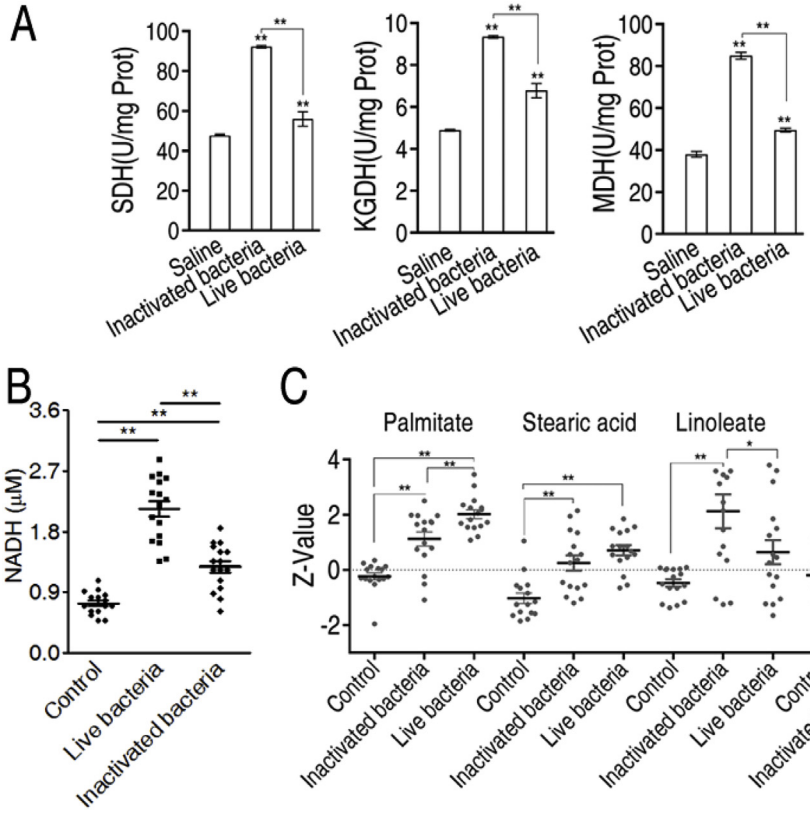

Fig. 5. The activity of enzymes in the TCA cycle, and levels of NADH and palmitic acid. (**A**) The activity of enzymes in the TCA cycle. (B) NADH levels of zebrafish after vaccination. (**C**) Palmitic acid levels based on GC-MS data among control, inactivated vaccine, and live vaccine. Each data point represents one technical repeat. All values are expressed as mean ± SEM (n = 8 per group). ** $P < 0.01$.

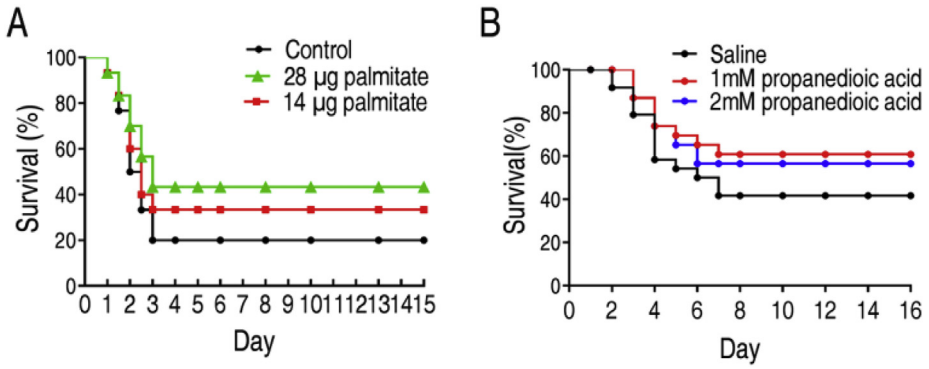

Fig. 6. Action of palmitate and propanedioic acid. (**A**) Percent survival of zebrafish in the presence of exogenous palmitate sodium. (**B**) Percent survival of zebrafish in the presence of exogenous propanedioic acid.

greater or equal to 0.019 and 0.40 for absolute value of covariance p and correlation p(corr), respectively. The variables responsible for discrimination between control and vaccination were shown in Fig. 4B and the enlargement of candidate biomarkers were displayed in Fig. 4C and D. It included fifteen negative correlation metabolites (*d*-glucuronolactone, L-alanine, 5-oxoproline, L-serine, L-tyrosine, L-lysine, L-valine, L-aspartate, L-proline, L-phenylalanine, L-glutamine, L-threonine, hypoxanthine, L-isoleucine and L-ornithine) (Fig. 4C) and eleven positive correlation metabolites (cholesterol, citrate, myo-inositol, palmitate, creatinine, oleate, stearate, malate, D-glucose, lactate and succinate) (Fig. 4D). Out of the negative and positive correlation metabolites, three (palmitate, oleate, stearate) belong to biosynthesis of unsaturated fatty acids, five (D-glucose, citrate, malate, lactate, succinate) were associated with carbohydrates metabolism, and twelve (L-alanine, L-serine, L-tyrosine, L-lysine, L-valine, L-aspartate, L-proline, L-phenylalanine, L-glutamine, L-threonine, L-isoleucine and L-ornithine) were associated with amino acids metabolism, respectively. These results suggest that these biomarkers provide an important clue to clarify immunometabolism elicited by inactivated *E. tarda* vaccine.

We assumed that crucial pathways containing biomarkers might play a critical role in the immunization. To test this idea, we classified biomarkers into crucial pathways. Biomarkers with negative covariance and relevant pathways were as follows. L-Alanine, L-Aspartate, L-Glutamine, L-Isoleucine, L-Lysine, L-Phenylalanine, L-Proline, L-Serine, L-Threonine, L-Tyrosine and L-Valine participated in aminoacyl-tRNA biosynthesis. L-Phenylalanine and L-Tyrosine participate in phenylalanine metabolism or phenylalanine, tyrosine, and tryptophan biosynthesis. L-Isoleucine, L-Threonine, and L-Valine participate in valine, leucine and isoleucine biosynthesis. Biomarkers with positive covariance and relevant pathways were as follows. Oleate, palmitate, and stearate belonged to biosynthesis of unsaturated fatty acids (including unsaturated and saturated fatty acids in the analytical software). Citrate, malate, and succinate belonged to the TCA cycle. D-glucose belonged to starch and sucrose metabolism. Metabolic flux network constructed by crucial pathways was listed in Fig. 4E. The network indicates that the elevated central carbon and biosynthesis of unsaturated fatty acids and

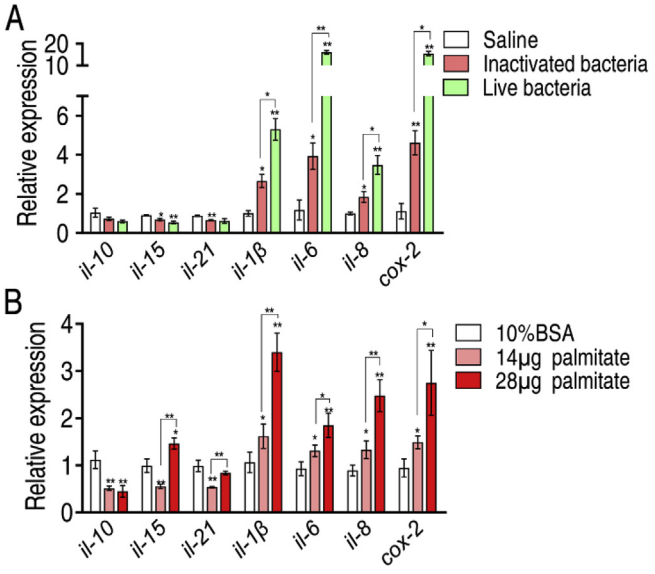

Fig. 7. QRT-PCR for expression of innate immune response genes in response to inactivated and live vaccines (A), and different concentrations of palmitate (B).

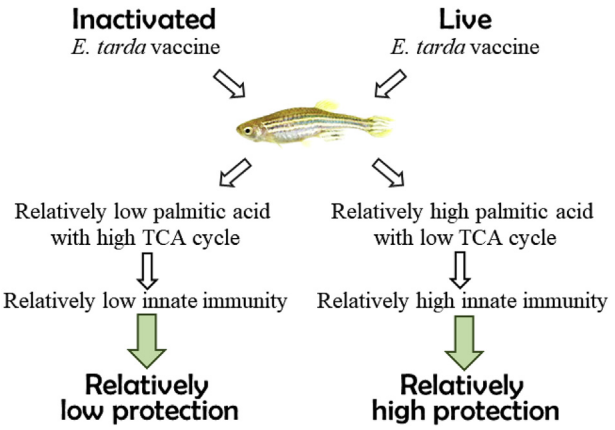

Fig. 8. A proposed model for a differential mechanism of live and inactivated *E. tarda* vaccines.

decreased amino acids form a characteristic feature in response to inactivated *E. tarda* vaccine.

3.5. Level of the elevated fatty acids is related to activity of the TCA cycle

The above data made us suppose that there is a relationship in the quantitative change between the TCA cycle and the biosynthesis of unsaturated fatty acids. Acetyl-CoA mainly fluxes to the TCA cycle and biosynthesis of fatty acids. The differential fluxes may balance the output between the two metabolic pathways. Thus, the activity of enzymes in the TCA cycle was measured. Results showed that both vaccines promote the activity of these enzymes, but higher activity was detected in inactivated vaccine than live vaccine (Fig. 5A). Correspondingly, inactivated vaccine stimulated higher NADH than live vaccine (Fig. 5B). Meanwhile, comparison in palmitic acid was performed between live vaccine and inactivated vaccine. In contrast, live vaccine promoted higher palmitate generation than inactivated vaccine (Fig. 5C). These results indicate that inactivated vaccine promotes more fuels to the TCA cycle and fewer fuels to biosynthesis of fatty acids, whereas live vaccine promotes fewer fuels to the TCA cycle and more fuels to biosynthesis of fatty acids.

3.6. Palmitate and propanedioic acid protect zebrafish from infections caused by E. tarda EIB202

The above data made us suppose that differential palmitic acid levels were related to the immune protection differences between live and inactivated vaccines. To demonstrate this, exogenous palmitate was intraperitoneally injected into zebrafish. These fish were challenged using EIB202. Immune protection was detected in zebrafish injected with palmitate with a dose-dependent manner (Fig. 6A), which indicates that elevation of palmitate increases survival ability of zebrafish against infections caused by EIB202. The metabolic flux of glycolysis and pyruvate metabolism goes to either the TCA cycle or biosynthesis of fatty acids. We supposed that slight inhibition of the TCA cycle makes more fuels to the biosynthesis of fatty acids and in turn increases the survival of zebrafish infected by EIB202. This was demonstrated by the addition of low concentration of propanedioic acid, which is an inhibitor of succinate dehydrogenase of the TCA cycle (Fig. 6B). These results indicate that the abundance of palmitate and the state of the TCA cycle is related to the immune protective ability.

3.7. Palmitate stimulates similar innate immunity with vaccines

To further demonstrate that the innate immunity stimulated by vaccines is mostly attributed to promotion of palmitate, expression of innate immunity genes was detected in response to live and inactivated vaccines, and different concentrations of palmitate. Both vaccines elevated expression of IL-1β, IL-6, IL-8, Cox-2 genes and inhibited expression of IL-10, IL-15, and IL-21 genes, where higher IL-1β, IL-6, IL-8, Cox-2 expression was found in live vaccine than inactivated vaccine (Fig. 7A). Similar expression of IL-1β, IL-6, IL-8, Cox-2 genes were detected in palmitate-injected zebrafish in a dose-dependent manner (Fig. 7B). These results indicate that high and low palmitate stimulate the differential innate immunities as live and inactivated vaccines do.

4. Discussion

Metabolomes modulate host's immunity against bacterial pathogens and bacterial sensitivity and resistance to antibiotics [18,32–38]. The present study used GC-MS based metabolomics to investigate the metabolic profile and identified metabolic characteristic features of zebrafish in response to inactivated *E. tarda* vaccine. Our results show that inactivated *E. tarda* vaccine is a potent metabolome modulator, which leads to the elevation of lipids and carbohydrates metabolisms and decrease of amino acids metabolism. Very recently, we have revealed that live *E. tarda* vaccine can modulate metabolome to combat infection caused by the bacterial pathogen. The modulated metabolome characterizes elevated biosynthesis of unsaturated fatty acids, which was further demonstrated to induce effective protection against *E. tarda* infection [19]. Compared with the data obtained from the live *E. tarda* vaccine, inactivated *E. tarda* vaccine modulates the similar metabolic profile as live *E. tarda* vaccine does. These findings support the conclusion that *E. tarda* vaccines promote innate immunity through metabolic modulation.

However, why similar metabolic profiles lead to differential immune protection, which challenges the relationship between innate immunity and metabolic modulation [18,21,24,39]. We supposed that abundance of key biomarkers is related to intensity of innate immunity. To explore this, a key biomarker, palmitate, was selected for further study. Consistent with stronger immune protection provided by live *E. tarda* vaccine, higher palmitate was detected in live vaccine than inactivated vaccine. The metabolite promoted zebrafish survival in a dose-dependent survival. Therefore, abundance of crucial biomarkers is responsible for differential capability in immune protection. These results support the above hypothesis that differential protection is attributed to differential abundance of a key biomarker in two similar metabolic profiles. The present study highlights a new way in

promotion of vaccine efficacy through modulating the abundance of key metabolites.

A question was raised whether innate responses induced by different concentrations of palmitate are in similar proportion to these mounted by inactivated and live vaccines. Our results showed that palmitate promotes expression of IL-1β, IL-6, IL-8, Cox-2 genes in a dose-dependent manner. Correspondingly, higher expression of IL-1β, IL-6, IL-8, Cox-2 genes was detected in live vaccine than inactivated vaccine. Thus, abundance of a key biomarker can regulate differential intensity of innate immunity and is responsible for differential survival. Palmitate induces IL-8 mRNA expression and secretion in a dose-dependent manner in human [40], which supports our findind that the live EIB202 vaccine induced higher immune response than inactivated vaccine. Palmitate induces IL-8 gene expression in human vascular smooth muscle cells through the TLR4/NF-κB pathway [40]. Thus, the pathway may be activated to regulate IL-8 gene expression in fish.

E. tarda is an intracellular pathogen causing severe economic loss in fish farming [1]. An understanding of anti-infective mechanisms against the bacterium is especially important in control of infection caused by the bacterial pathogen for food safety and human health. A line of evidence has indicated the importance of innate immunity and adaptive immunity in anti-infective action [41–43]. We have recently demonstrated metabolic modulation plays a key role in live vaccine-induced immunity [19]. In exploring the metabolic modulation mechanisms by which fish develop innate immunity against *E. tarda* infection, we showed that upregulation and downregulation abundances of glucose are characteristic features in survival-metabolome and death-metabolome, respectively [20]. Exogenous glucose promotes biosynthesis of fatty acids and elevates fish survival, indicating that glucose reduces host's death caused by *E. tarda* infection through increased biosynthesis of fatty acids [21]. Like the survival-metabolome, elevated glucose and palmitate are identified in both live and inactivated vaccines-induced metabolomes [19] (data of the present study). These results strongly support the conclusion that *E. tarda* vaccines modulate metabolome that characterizes elevation of carbohydrate metabolism and biosynthesis of fatty acids to display immunoprophylaxis effect. These findings provide useful biomarkers for the development of *E. tarta* vaccines, where glucose and biosynthesis of fatty acids can be biomarkers to evaluate the efficacy of vaccines. Furthermore, our results have been implicated in evaluation of other vaccines through identification of valuable metabolic biomarkers. Whether other vaccines promote similar abundanc of palmic acid to regulate the differential immune protection waits further investigation. However, our recent results have shown when fish were infected with sub-lethal dose of *V. alginolyticus* V12G01, dying fish and the survival fish exhibit differential metabolomes. The metabolomes characterize with elevated stearic acid and palmitic acid and attenuated TCA cycle in dying fish but decreased stearic acid and palmitic acid and elevated TCA cycle [44]. Therefore, different biomarkers may be identifid from diverse bacterial vaccines.

Based on these findings, *E. tarda* pathogenesis is proposed as shown in Fig. 8. When fish hosts were injected with live and inactivated vaccines, carbohydrates metabolisms are differentially impacted. Both promote the TCA cycle and biosynthesis of fatty acids, but live vaccine stimulates lower TCA cycle and higher biosynthesis of palmitic acid than inactivated vaccine. Consistently, both activate innate immunity, but live vaccine stimulates higher innate immune response than inactivated vaccine. Thus, live EIB202 vaccine provides higher immune response than inactivated vaccine.

In summary, the present study aims to investigate whether metabolic modulation contributes to the immune protection of inactivated vaccines. Our results demonstrate that live *E. tarda* vaccine promotes higher biosynthesis of palmitic acid, which provides zebrafish for protection against EIB202 infection. The metabolic characteristics displayed by the inactivated vaccine are similar as those possessed by live vaccine and EIB202 challenge, but the abundance of crucial biomarkers such as palmitate is lower, which leads to lower immune protection against infection caused by *E. tarda*.

Acknowledgments

This work was sponsored by grants from the National Key Research and Development Plan (2016YFD0501307) and NSFC projects (31572654, 31772888).

References

[1] X. Liu, X. Chang, H. Wu, J. Xiao, Y. Gao, Y. Zhang, Role of intestinal inflammation in predisposition of *Edwardsiella tarda* infection in zebrafish (*Danio rerio*), Fish Shellfish Immunol. 41 (2) (2014) 271–278.
[2] S. Shinyoshi, Y. Kamada, K. Matsusaki, P.K. Chigwechokha, S. Tepparin, K. Araki, M. Komatsu, K. Shiozaki, Naringenin suppresses Edwardsiella tarda infection in GAKS cells by NanA sialidase inhibition, Fish Shellfish Immunol. 61 (2017) 86–92.
[3] L. Sun, H. Chen, W. Lin, X. Lin, Quantitative proteomic analysis of Edwardsiella tarda in response to oxytetracycline stress in biofilm, J. Proteomics 150 (2017) 141–148.
[4] H. Venter, M.L. Henningsen, S.L. Begg, Antimicrobial resistance in healthcare, agriculture and the environment: the biochemistry behind the headlines, Essays Biochem. 61 (2017) 1–10.
[5] K. Sun, H.L. Wang, M. Zhang, Z.Z. Mao, L. Sun, Genetic mechanisms of multi-antimicrobial resistance in a pathogenic *Edwardsiella tarda* strain, Aquaculture 289 (2009) 134–139.
[6] J.E. Yu, M.Y. Cho, J.W. Kim, H.Y. Kang, Large antibiotic-resistance plasmid of Edwardsiella tarda contributes to virulence in fish, Microb. Pathog. 52 (5) (2012) 259–266.
[7] Y. Du, X. Tang, X. Sheng, J. Xing, W. Zhan, The influence of concentration of inactivated *Edwardsiella tarda* bacterin and immersion time onantigen uptake and expression of immune-related genes in Japanese flounder (*Paralichthys olivaceus*), Microb, Pathogens 103 (2017) 19–28.
[8] X.H. Liu, J.M. Xu, H. Zhang, Q. Liu, J.F. Xiao, Y.X. Zhang, Design and evaluation of an *Edwardsiella tarda* DNA vaccine co-encoding antigenic and adjuvant peptide, Fish Shellfish Immunol. 59 (2016) 189–195.
[9] C. Wang, Y.H. Hu, H. Chi, L. Sun, The major fimbrial subunit protein of *Edwardsiella tarda*: vaccine potential, adjuvant effect, and involvement in host infection, Fish Shellfish Immunol. 35 (2013) 858–865.
[10] Y.J. Yan, W. Mu, L.Z. Zhang, L.Y. Guan, Q. Liu, Y.X. Zhang, Asd-based balanced-lethal system in attenuated *Edwardsiella tarda* to express a heterologous antigen for a multivalent bacterial vaccine, Fish Shellfish Immunol. 34 (2013) 1188–1194.
[11] E.J. Sayour, D.A. Mitchell, Manipulation of innate and adaptive immunity through cancer vaccines, J. Immunol Res. 2017 (2017) 3145742.
[12] A. Egli, D. Santer, K. Barakat, M. Zand, A. Levin, M. Vollmer, M. Weisser, N. Khanna, D. Kumar, L. Tyrrell, M. Houghton, M. Battegay, D. O'Shea, Vaccine adjuvants-understanding molecular mechanisms to improve vaccines, Swiss Med. Wkly. 144 (2014) w13940.
[13] T. Wang, C.J. Secombes, The cytokine networks of adaptive immunity in fish, Fish Shellfish Immunol. 35 (6) (2013) 1703–1718.
[14] M. Yamasaki, K. Araki, K. Maruyoshi, M. Matsumoto, C. Nakayasu, T. Moritomo, T. Nakanishi, A. Yamamoto, Comparative analysis of adaptive immune response after vaccine trials using live attenuated and formalin-killed cells of Edwardsiella tarda in ginbuna crucian carp (Carassius auratus langsdorfii), Fish Shellfish Immunol. 45 (2) (2015) 437–442.
[15] X. Liu, H. Zhang, C. Jiao, Q. Liu, Y. Zhang, J. Xiao, Flagellin enhances the immunoprotection of formalin-inactivated *Edwardsiella tarda* vaccine in turbot, Vaccine 35 (2017) 369–374.
[16] M. Boothby, R.C. Rickert, Metabolic regulation of the immune humoral response, Immunity 46 (2017) 743–755.
[17] T. Young, Andrea C. Alfaro, Metabolomic strategies for aquaculture research: a primer, Rev. Aquacult. 0 (2016) 1–31, https://doi.org/10.1111/raq.12146.
[18] X.H. Chen, S.R. Liu, B. Peng, D. Li, Z.X. Cheng, J.X. Zhu, S. Zhang, Y.M. Peng, H. Li, T.T. Zhang, X.X. Peng, Exogenous L-valine promotes phagocytosis to kill multidrug-resistant bacterial pathogens, Front. Immunol. 8 (2017) 207.
[19] C. Guo, B. Peng, M. Song, C.W. Wu, M.J. Yang, J.Y. Zhang, H. Li, Live *Edwardsiella tarda* vaccine enhances innate immunity by metabolic modulation in zebrafish, Fish Shellfish Immunol. 47 (2015) 664–673.
[20] B. Peng, Y.M. Ma, J.Y. Zhang, H. Li, Metabolome strategy against *Edwardsiella tarda* infection through glucose-enhanced metabolic modulation in *tilapias*, Fish Shellfish Immunol. 45 (2) (2015) 869–876.
[21] Z.H. Zeng, C.C. Du, S.R. Liu, H. Li, X.X. Peng, B. Peng, Glucose enhances tilapia against *Edwardsiella tarda* infection through metabolome reprogramming, Fish Shellfish Immunol. 61 (2017) 34–43.
[22] Q.Y. Wang, M.J. Yang, J.F. Xiao, H.Z. Wu, X. Wang, Y.Z. Lv, L.L. Xu, H.J. Zheng, S.Y. Wang, G.P. Zhao, Q. Liu, Y.X. Zhang, Genome sequence of the versatile fish pathogen *Edwardsiella tarda* provides insights into its adaptation to broad host ranges and intracellular niches, PLoS One 4 (2009) e7646.
[23] C. Guo, X.Y. Huang, M.J. Yang, S. Wang, S.T. Ren, H. Li, X.X. Peng, GC/MS-based metabolomics approach to identify biomarkers differentiating survivals from death in crucian carps infected by *Edwardsiella tarda*, Fish Shellfish Immunol. 39 (2014) 215–222.

[24] X.L. Zhao, C.W. Wu, X.X. Peng, H. Li, Interferon-α2b against microbes through promoting biosynthesis of unsaturated fatty acids, J. Proteome Res. 13 (2014) 4155–4163.
[25] T. Kind, K.H. Liu, Do Y. Lee, B. DeFelice, J.K. Meissen, O. Fiehn, LipidBlast in silico tandem mass spectrometry database for lipid identification, Nat. Methods 10 (2013) 755–758.
[26] K.L. Busch, Units in mass spectrometry, Spectroscopy 16 (2001) 28–31.
[27] A. Sreekumar, L.M. Poisson, T.M. Rajendiran, A.P. Khan, Q. Cao, J. Yu, et al., Metabolomic profiles delineate potential role for sarcosine in prostate cancer progression, Nature 457 (2009) 910–914.
[28] J.D. Storey, A direct approach to false discovery rates, J. R. Stat. Soc. B 64 (2002) 479–498.
[29] J. Xia, R. Mandal, I.V. Sinelnikov, D. Broadhurst, D.S. Wishart, MetaboAnalyst 2.0-a comprehensive server for metabolomic data analysis, Nucleic Acids Res. 40 (2012) W127–W133.
[30] S.R. Liu, X.X. Peng, H. Li, Metabolic mechanism of ceftazidime resistance in *Vibrio alginolyticus*, Infect. Drug Resist. 12 (2019) 417–429.
[31] Y. Wang, X. Wang, F. Ali, Z. Li, Y. Fu, X. Yang, W. Lin, X. Lin, Comparative extracellular proteomics of *Aeromonas hydrophila* reveals iron-regulated secreted proteins as potential vaccine candidates, Front. Immunol. 10 (2019) 256.
[32] Z.J. Yao, W.X. Li, Y. Lin, Q. Wu, F.F. Yu, W.X. Lin, X.M. Lin, Proteomic analysis reveals that metabolic flows affect the susceptibility of *Aeromonas hydrophila* to antibiotics, Sci. Rep. 6 (2016) 39413 e1-10.
[33] J. Yang, Z.H. Zeng, M.J. Yang, Z.X. Cheng, X.X. Peng, H. Li, NaCl promotes antibiotic resistance by reducing redox states in *Vibrio alginolyticus*, Environ. Microbiol. 20 (2018) 4022–4036.
[34] M. Jiang, Q.Y. Gong, S.S. Lai, Z.X. Cheng, Z.G. Chen, J. Zheng, B. Peng, Phenylalanine enhances innate immune response to clear ceftazidime-resistant *Vibrio alginolyticus* in *Danio rerio*, Fish Shellfish Immunol. 84 (2019) 912–919.
[35] Z.X. Cheng, M.J. Yang, B. Peng, X.X. Peng, X.M. Lin, H. Li, The depressing central carbon and energy metabolisms mediate levofloxacin resistance in *Vibrio alginolyticus*, J. Proteomics 181 (2018) 83–91.
[36] Z. Yao, Z. Guo, Y. Wang, W. Li, Y. Fu, Y. Lin, W. Lin, X. Lin, Integrated succinylome and metabolomics reveals lysine succinylated LuxS plays a crucial role in quorum sensing and metabolism of *Aeromonas hydrophila*, Mol. Cell. Proteom. 18 (2019) 200–215.
[37] J.Z. Ye, Y.B. Su, X.M. Lin, S.S. Lai, W.X. Li, F. M Ali, J. Zheng, B. Peng, Alanine enhances aminoglycosides-induced ROS production as revealed by proteomic analysis, Front. Microbiol. 9 (2018) 29.
[38] J.Z. Ye, X.M. Lin, Z.X. Cheng, Y.B. Su, W.X. Li, F.M. Ali, J. Zheng, B. Peng, Identification and efficacy of glycine, serine and threonine metabolism in potentiating kanamycin-mediated killing of *Edwardsiella piscicida*, J. Proteomics 183 (2018) 34–44.
[39] Z.X. Cheng, Q.Y. Gong, Z. Wang, Z.G. Chen, J.Z. Ye, J. Li, J. Wang, M.J. Yang, X.P. Lin, B. Peng, *Edwardsiella tarda* tunes tricarboxylic acid cycle to evade complement-mediated killing, Front. Immunol. 8 (2017) 1706.
[40] X.H. Chen, B.W. Zhang, H. Li, X.X. Peng, Myo-inositol improves the host's ability to eliminate balofloxacin-resistant, Sci. Rep. 5 (2015) 10720.
[41] A.C. Alfaro, T. Young, Showcasing metabolomic applications in aquaculture: a review, Rev. Aquacult. 10 (2016) 1–18.
[42] J. Quan, J. Liu, X. Gao, J. Liu, H. Yang, W. Chen, W. Li, Y. Li, W. Yang, B. Wang, Palmitate induces interleukin-8 expression in human aortic vascular smooth muscle cells via Toll-like receptor 4/nuclear factor-κB pathway (TLR4/NF-κB-8), J. Diabetes 6 (2014) 33–41.
[43] Y.J. Hsu, C.Y. Hou, S.J. Lin, W.C. Kuo, H.T. Lin, J.H. Lin, The biofunction of orange-spotted grouper (Epinephelus coioides) CC chemokine ligand 4 (CCL4) ininnate and adaptive immunity, Fish Shellfish Immunol. 35 (2013) 1891–1898.
[44] M.J. Yang, Z.X. Cheng, M. Jiang, Z.H. Zeng, B. Peng, X.X. Peng, H. Li, Boosted TCA cycle enhances survival of zebrafish to *Vibrio alginolyticus* infection, Virulence 9 (2018) 634–644.